International Journal on
"Technical and Physical Problems of Engineering"
(IJTPE)
Published by International Organization of IOTPE

ISSN 2077-3528
IJTPE Journal
www.iotpe.com
ijtpe@iotpe.com

March 2022	Issue 50	Volume 14	Number 1	Pages 42-49

STRUCTURE OPTIMIZATION OF A HEXAPOD ROBOT

M. Atify [1] M. Bennani [2] A. Abouabdellah [1]

1. Laboratory of Engineering Science (LSI) ENSA, Ibn Tofail University, Kenitra, Morocco
atifym@gmail.com, a.abouabdellah2013@gmail.com
2. Laboratory of Mechanics and Industrial Processes and Process (LM2PI), ENSAM, Mohamed V University, Rabat, Morocco, m.bennani@um5s.net.ma

Abstract- The study carried out concerns the optimization of the parameters of a hexapod robot. It focuses on the stability performance in terms of stability margins of the robot during the propelling phase. Also, the mobility of the robot is an important criterion for the optimization process. This aspect is well developed in the study. Many structure parameters of the hexapod are considered such as the gait type, the hexapod's body, the length legs, the body height and the contact positions of the legs. The geometric model is established to be used in the global platform of simulation which numerically solve it. Biological models of insects are taken to choose some structure parameters of the hexapod robot. They constitute valuable data to be used in an artificial intelligence program. Therefore, an efficient procedure is applied to validate the good structures according the extent of the robot's workspace and the degree of the stability margin.

Keywords: Hexapod, Geometric Modeling, Optimization, Stability, Workspace, Artificial Intelligence.

1. INTRODUCTION

Robots are classified into two broad categories [1], stationary robots and walking robots. Among the stationary robots we find serial robots and parallel robots [2]. For walking robots, a distinction is made between simple [3] or multidirectional wheeled robots, crawler robots [4], [5], [6], hybrid robots [7], [8], [9], and legged robots. Each type of robots has its advantages and disadvantages. In our study we are interested in walking robots with 6 legs, which have more stability compared to robots with 1 leg [10], 2 legs [11], [12], [11], [13], or even 4 legs [14], [15]. These hexapod robots have the major advantage, to move on uneven terrains. But in return their mobility is limited and their gait control is often complicated.

Geometric studies of hexapods have been dealt with in studies [17], [18], and [19]. Kinematic studies are also treated in hexapod robots according to the adopted gait [20], [21], [22]. Many uses of the Denavit-Hartenberg representation [23], [24], are also considered to establish the direct and inverse kinematic models.

Important robotics researches are based on biological models from insects and animals. The cockroach's tripod gait is considered in [25] while the tetrapod gait [26] is adopted to underline the good performance of the African ostrich. In [27] is treated the case of a hexapod robot inspired by an ant with measurements of the ant shape.

The movement of a locust by its leg is studied in [28], [29] Treated the overturning of the ladybug according to several parameters. An interesting work is achieved in [30] to analyze the influence of hydrodynamics aspect on the displacement of a crab.

The stability aspect of the legged robots is considered by many researchers due to its importance. The static stability margins of a legged robot are used in [37], [38], [39]. A Simulink platform is developed in [40,] to study the stability of a hexapod robot. Also, the stability is analyzed in the case of a tripod walk of a hexapod robot [41], [42]. Analyzed the stability by the minimum energy required to fall a robot (Energy Stability Margin). [43] Studied the stability for walking robots by defining the Normalized Dynamic Energy Stability Margin. Which is the smallest of the stability levels required to tumble the robot around the support polygon. [44] Used sensors measuring the forces at the contacts between the robot and the ground for the calculation of Foot Force Stability Margin (FFSM). [45] Also analyzed the stability by FFSM for walking robots.

Our work is based on the optimization of the parameters of the robot according to the possible displacement distance, the stability parameters and the desired displacement distance. We also take into account the interference of the legs during the propelling and the lifting phases in the adopted gait. This paper is organized by a presentation of the hexapod robot with all its interesting parameters. It's followed in section III by a modeling part. It determines the workspace and the stability of the hexapod by specific measurements. Then section IV proposes a numerical approach used with an algorithm of neural networks which exhibit some meaningful results finally, a conclusion with some perspectives is given.

2. PRESENTATION

The hexapod robot used is made up of a body of the length L_b, the width d_b, the height e_b and the offset d_p. The body is linked with six legs L_i $(i = 1...6)$, by pivot links respectively at points D_i arranged in the order given in Figure 1.

In Figure 2, each leg is formed by three segments (thigh, tibia and the foot). The thigh is of length L_{i1} in pivot connection with the body at the point D_i. It has also a pivot connection in C_i with the Tibia. The Tibia, of length L_{i2} is in pivot joint in B_i with the foot. The foot is posed in the ground at the point A_i.

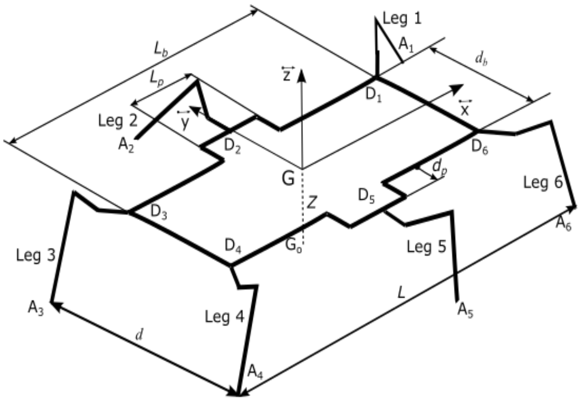

Figure 1. Presentation of the robot

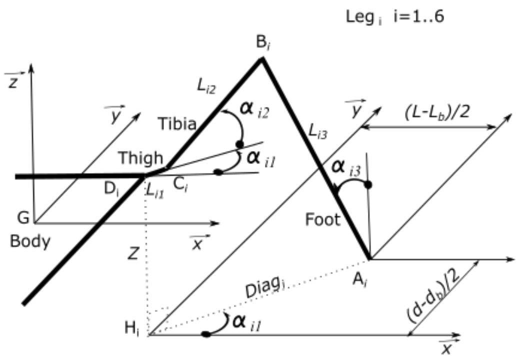

Figure 2. Presentation of a leg

3. MODELING

3.1. Workspace

The workspace of a hexapod robot is developed in [46], which illustrates the space described by the center of inertia of the robot during its motion. The study is made in the space according the Figures 3a and 3b and also in a horizontal plane located at a very precise height in Figures 3c and 3d.

The expression of this workspace in a plane is called a Workplan. It depends on the displacement height of the robot's body with respect to the ground noted *Z*. The hind legs of Leg3, Leg4, and the positions of the contacts points between the robot and the ground involve the angles of inclination of different parts of the legs.

The maximum displacement following longitudinal axis $\vec{x}$, denoted by W_x, is given by the Equation (1) [46]. The Figures 3a [46] and 3b [46] show an example of workspace represented in space in two different views. The others Figures 3c [46] and 3d [46] represent the Workplan at 2 different heights.

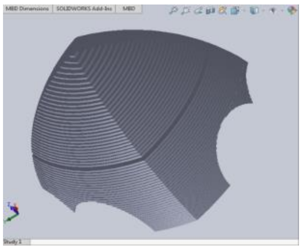

a) in space in profile view

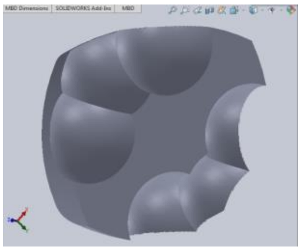

b) in space in rear view

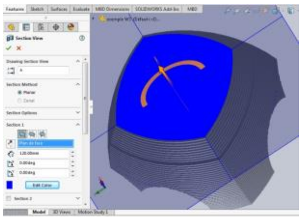

c) in a plane located at a height

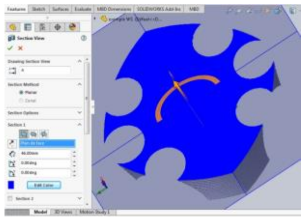

d) in a plane located at other height

Figure 3. An example of workspace [46]

The expression of the workspace indicator is established as follows [46]:

$$W_x = \sqrt{(\sqrt{(L_{42}+L_{43})^2 - Z^2} + L_{41})^2 - \left(\frac{d-d_b}{2}\right)^2} - \left(\frac{L-L_b}{2}\right) \quad (1)$$

From Figure 2:

we can determine the terms $\left(\frac{L-L_b}{2}\right)$ and $\left(\frac{d-d_b}{2}\right)$ as a function of αij as:

$$\left(\frac{L-L_b}{2}\right) = Diag_4 \cos\alpha_{41} \quad (2)$$

$$\left(\frac{d-d_b}{2}\right) = Diag_4 \sin\alpha_{41} \quad (3)$$

$$Diag_4 = L_{41} + L_{42}\cos\alpha_{42} + L_{43}\sin\alpha_{43} \quad (4)$$

Therefore, we deduce:

$$W_x = \sqrt{(\sqrt{(L_{42}+L_{43})^2 - Z^2} + L_{41})^2 - ...}$$
$$\sqrt{(... - (L_{41} + L_{42}\cos\alpha_{42} + L_{43}\sin\alpha_{43})^2 \sin^2\alpha_{41}} - \quad (5)$$
$$-((L_{41} + L_{42}\cos\alpha_{42} + L_{43}\sin\alpha_{43})\cos\alpha_{41})$$

3.2. Desired Displacement of the Robot Body

During movement, the robot can perform a displacement W_x, which depends mainly on the lengths of the hind legs 3 and 4, according to Equation (5). It can only move to a desired distance S_x which must be less or equal to W_x.

For this reason, we have to check that all the legs will be able to achieve this desired displacement S_x. It depends on the parameters α_{ij}, Z and the dimensions of the robot. Therefore, it requires finding the best values of these position parameters for each leg. The Figure 4, shows a configuration where W_x is much less than S_x. In this case the robot cannot travel the distance S_x, because the movement limit is W_x. The Figure 5 shows that W_x is much greater than S_x. In this case the robot will only perform a small displacement S_x although the leg positions can reach the large displacement W_x.

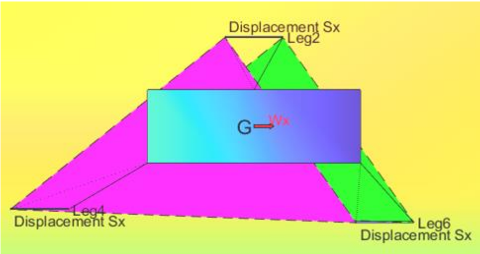

Figure 4. Case where W_x much less than S_x

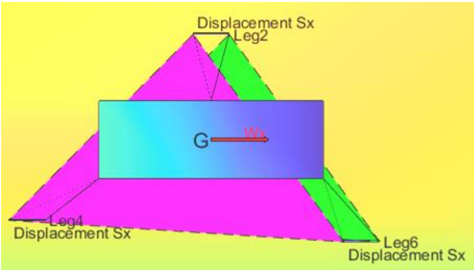

Figure 5. Case where W_x much greater than S_x

3.2.1. The Positions of the Leg 6

The contact point A_6 of leg 6 with the ground has the coordinates: A_6x along the $\vec{x}$ axis and A_6y along the $\vec{y}$ axis. The coordinates of the point of articulation D_6 of leg 6 with the robot body are: D_6x along the $\vec{x}$ axis and D_6y along the $\vec{y}$ axis.

In the starting position of the leg 6, and using parameters in Figure 2, we obtain:

$$A_6x - D_6x = (L_{61} + L_{62}\cos\alpha_{62} + L_{63}\sin\alpha_{63})\cos\alpha_{61} \quad (6)$$

$$A_6y - D_6y = (L_{61} + L_{62}\cos\alpha_{62} + L_{63}\sin\alpha_{63})\sin\alpha_{61} \quad (7)$$

$$Z = L_{63}\cos\alpha_{63} - L_{62}\sin\alpha_{62} \quad (8)$$

Considering S_x the longitudinal displacement of the robot body along the $\vec{x}$ axis, the point D_6 also moves by the same distance S_x. So, the final position of leg 6 will be given by the following relations by adding "f" which designates final, to the position parameters of the leg.

$$A_6x - D_6x_f = A_6x - (D_6x + S_x) = \\ = (L_{61} + L_{62}\cos\alpha_{62f} + L_{63}\sin\alpha_{63f})\cos\alpha_{61f} \quad (9)$$

$$A_6y - D_6y_f = (L_{61} + L_{62}\cos\alpha_{62f} + L_{63}\sin\alpha_{63f})\sin\alpha_{61f} \quad (10)$$

$$Z = L_{63}\cos\alpha_{63f} - L_{62}\sin\alpha_{62f} \quad (11)$$

3.2.2. The Positions of the Leg 2

The contact point A_2 of leg 2 with the ground has the coordinates: A_2x along the $\vec{x}$ axis and A_2y along the $\vec{y}$ axis. We note also the coordinates of the point of articulation D_2 of leg 2 with the robot body which are: D_2x along the $\vec{x}$ axis and D_2y along the $\vec{y}$ axis.

In the starting position of the leg 2, and using also the parameters of the Figure 2 leads to:

$$A_2x - D_2x = (L_{21} + L_{22}\cos\alpha_{22} + L_{23}\sin\alpha_{23})\cos\alpha_{21} \quad (12)$$

$$A_2y - D_2y = (L_{21} + L_{22}\cos\alpha_{22} + L_{23}\sin\alpha_{23})\sin\alpha_{21} \quad (13)$$

$$Z = L_{23}\cos\alpha_{23} - L_{22}\sin\alpha_{22} \quad (14)$$

Considering the same longitudinal displacement along the $\vec{x}$ axis: S_x, and the same notation "f" used in the case of leg 6, the final position of the leg 2 will be given by:

$$A_2x - D_2x_f = A_2x - (D_2x + S_x) = \\ (L_{21} + L_{22}\cos\alpha_{22f} + L_{23}\sin\alpha_{23f})\cos\alpha_{21f} \quad (15)$$

$$A_2y - D_2y_f = (L_{21} + L_{22}\cos\alpha_{22f} + L_{23}\sin\alpha_{23f})\sin\alpha_{21f} \quad (16)$$

$$Z = L_{23}\cos\alpha_{23f} - L_{22}\sin\alpha_{22f} \quad (17)$$

Legs 2 and 5 must follow the movement of the robot body such as for the legs 1 and 6. Geometrically, legs 1 and 6 were in their initial positions during the body movement. They start to bend because the robot's body approaches the point of contact of the leg with the ground. It's the same for the legs 2 and 5 which bend and lengthen without exceeding the dimensions of the initial position. This is, unlike the legs 3 and 4 which are lengthening, since the robot's body moves away from the initial contact point.

3.3. Stability

3.3.1. Propulsion with 3 legs

The problem of stability arises in particular for a propelling with 3 legs. We suppose that the lifting is done with the legs 1, 3 and 5. Therefore, there is no contact between these legs and the ground. The propelling will be done with legs 2, 4 and 6 which remain in contact with the ground. In order for the robot to be stable, it must be ensured, during the movement that the center of mass (COM) remains inside the stability polygon formed by the triangle A_2, A_4 and A_6.

In Figure 6, the COM G is placed inside the triangle of stability at the start of the propelling. The configuration of the robot in Figure 7, shows that the COM is still, inside the stability polygon, until the end of the movement. In figure 8 shows a superposition of the configurations from the start to the end of the movement. The start of the movement is shown in dotted lines while the configuration at the end of the movement is shown in solid lines.

Figure 9 shows an unstable configuration of the robot before moving. The propelling is made by legs 2, 4 and 6, since the COM G is placed outside the stability polygon formed by A_2, A_4 and A_6.

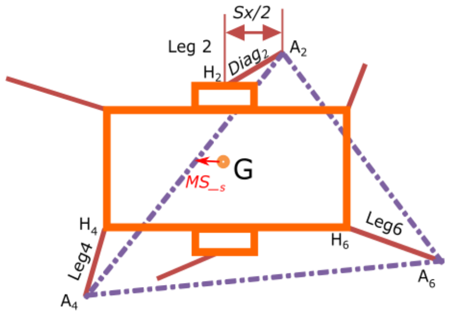

Figure 6. Stability at the start of the propelling

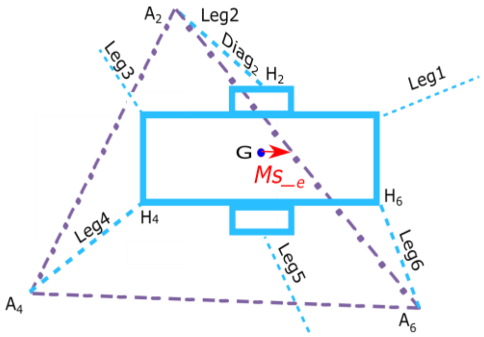

Figure 7. Stability at the end of the movement

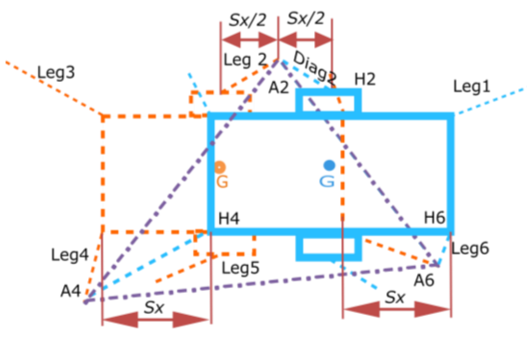

Figure 8. Stability from start to finish of movement

An unstable configuration at the end of the movement is shown in Figure 10, with the position of COM G in outside of the stability polygon A_2, A_4 and A_6.

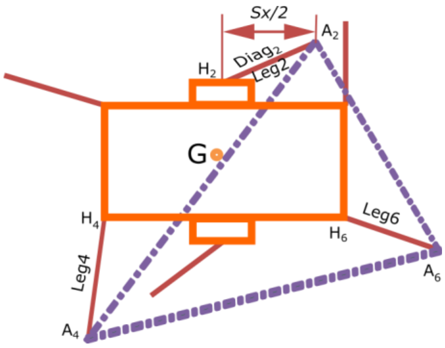

Figure 9. Instability at the start of the movement

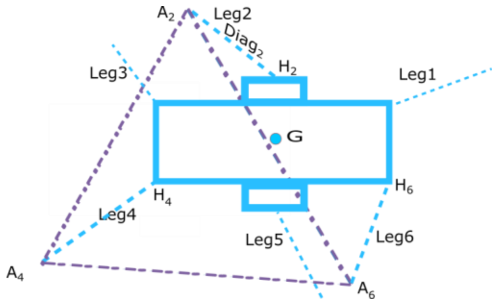

Figure 10. Instability at the end of the movement

3.3.3. Margins of Stability

The stability margin is a distance measured on the longitudinal axis of the robot between the position of the center of mass G and the stability triangle for a stable robot. We deduce that with a greater stability margin, the robot would be more stable.

The coordinates of the initial points A_2, A_4 (before displacement) with respect to the initial position of the COM G, projected in the horizontal plane ($\vec{x}, \vec{y}$) are respectively A_2x, A_4x along the $\vec{x}$ axis, and A_2y, A_4y along the axis $\vec{y}$.

The coordinates of the end points A_2, A_6 (after displacement) with respect to the initial position of the COM G, projected in the horizontal plane ($\vec{x}, \vec{y}$) are respectively A_2x_f, A_6x_f along the $\vec{x}$ axis, and A_2y_f, A_6y along the axis $\vec{y}$.

The calculation of the stability margin is established before moving. So, the equation of the left segment of triangle $A_2\ A_4$ becomes:

$$y = \left(\frac{A_2y - A_4y}{A_2x - A_4x}\right)(x - A_2x) + A_2y \quad (18)$$

We put:

$$AA_{\_s} = \left(\frac{A_2y - A_4y}{A_2x - A_4x}\right);\ BB_{\_s} = \left(\frac{A_2xA_4y - A_2yA_4x}{A_2x - A_4x}\right) \quad (19)$$

For $x = 0$, if $y(0) > 0$ (also $BB_{\_s}$ >0) then the robot is stable. The stability margin before displacement is:

$$MS_{\_s} = (BB_{\_s} / AA_{\_s}) \quad (20)$$

After displacement, the equation of the right segment of triangle $A_2\ A_6$ is given by:

$$y = \left(\frac{A_2y_f - A_6y_f}{A_2x_f - A_6x_f}\right)(x - A_2x_f) + A_2y_f \quad (21)$$

We then put:

$$AA_{\_e} = \left(\frac{A_2y_f - A_6y_f}{A_2x_f - A_6x_f}\right)$$
$$BB_{\_e} = \left(\frac{A_2x_fA_6y_f - A_2y_fA_6x_f}{A_2x_f - A_6x_f}\right) \quad (22)$$

For $x = 0$, if $y(0) > 0$ (also $BB_{\_e}$ >0) then the robot is stable. The stability margin is established after the motion is described by:

$$MS_{\_e} = (BB_{\_e} / AA_{\_e}) \quad (23)$$

4. RESOLUTION

4.1. Resolution Approach

Taking into account the complexity of the analysis of the optimization parameters, a numerical resolution is established by a program that takes into account the constraints of stability of the robot and its margins, based on the Equations (20), and (23). It takes into account the possible displacement of the robot: W_x, given by Equation (5), for a given configuration. A check of the real displacement S_x is made which must be less than the possible displacement by the robot W_x. In these configurations the legs 2 and 6 must follow the displacement while respecting the Equations (9), (10), (11), (15), (16), and (17).

A graphical interface, in Figure 11, is made to enter the information necessary for the study. The result is obtained in Figure 12, which shows the stability before displacement by a green triangle and the stability at the end of the displacement represented by a blue triangle. The possible displacement on the longitudinal axis is represented by a red arrow W_x. In the other hand the displacement S_x, the margins of stability $MS_{\_s}$ and $MS_{\_e}$, in addition to the positions of the legs (before the displacement) are plotted in solid lines. We also note the positions of these legs at the end of the movement in dotted lines.

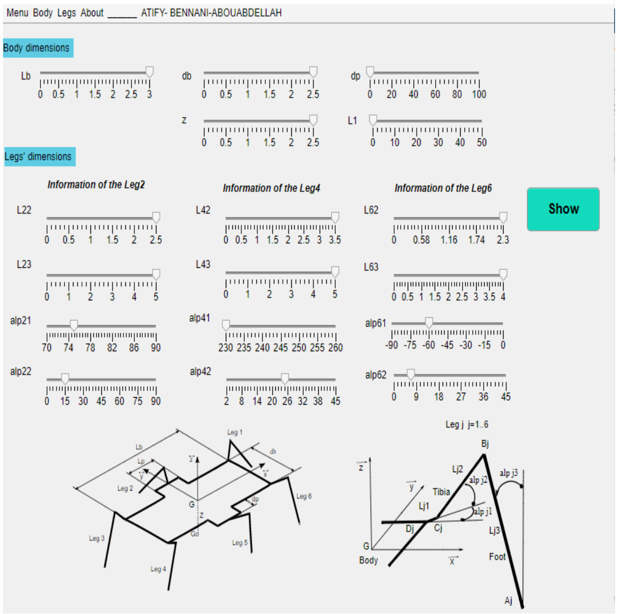

Figure 11. GUI interface for introducing information

The verification of the program and the validation of the established results found are done by using the real dimensions of the ants [48], [49], [50], [51].

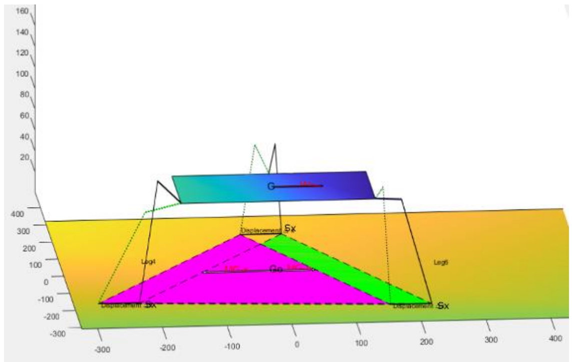

Figure 12. Example of the results

4.2. Artificial Intelligence Approach

In order to optimize the robot's movement parameters according the large number of parameters related to its movement, the use of artificial intelligence [52], [53], would be of great interest. The inputs to the algorithm are chosen by analogy to insect movements, that is, the dimensions of the insect and the lengths of the legs are known. For a desired six movement, the insect must position its legs well to propel. Our approach consists in following the same procedure to determine many factors: the α_{ij}, which gives the positions of the points of contact with the ground, the height Z of displacement of the body, the possible displacement W_x, and the margins of stability $MS_{\_s}$ and $MS_{\_e}$.

A database includes an input table (InputData) in table 1, which contains 10 input variables: L_b, d_b, d_p, L_{ij} and S_x. The output table (OutputData) in table 2 contains 10 outputs: α_{ij}, Z, W_x, $MS_{\_s}$ and $MS_{\_e}$. The values of this database are obtained from the configurations which are optimized, verified and validated by the initial program. The neural network algorithm is built from 70% of the database for learning, 15% of that base for validation, and 15% for testing.

The learning phase is carried out on the results found by the initial program for the combinations which are optimal, according to the information in the input table and the output table.

A training of the neural network is established, figure 13, to build the network and consequently, it determines the coefficients of the weights and the biases. The performance of the network is checked by the Mean Squared Error (MSE).

Table 1. Sample of the database entries

L_b	d_b	d_p	L_{22}	L_{23}	L_{42}	L_{43}	L_{62}	L_{63}	S_x
300	160	30	70	120	70	120	70	120	76.6
300	160	40	70	120	82	126	40	108	74.5
250	160	70	65	116	95	160	50	100	76.6
300	100	0	70	120	70	120	70	120	83.4
300	70	0	70	120	70	120	70	120	83.4
250	160	70	65	116	95	160	50	100	76.6
50	160	0	70	120	70	120	70	120	83.4
100	160	0	70	120	70	120	70	120	83.4
50	160	0	70	120	70	120	70	120	83.4
300	50	0	70	120	70	120	70	120	83.4
200	160	80	65	116	95	160	50	100	76.6

Table 2. Output database

Z	α_{21}	α_{22}	α_{41}	α_{42}	α_{61}	α_{62}	W_x	MS_{-s}	MS_{-e}
80	74	15	230	24.5	-60	6.5	77	116.5	62.6
93	71	14	254	8	-40	6	75	67.3	55
86	71	13	246	19	-41	6	78.8	83.6	64.7
65	72	26	255	25	-60	6	83.6	70.3	50
65	72	26	255	25	-60	6	83.6	70.2	49.6
86	71	13	246	19	-41	6	78.8	83.6	64.7
65	72	26	255	25	-60	6	83.6	33.5	14.2
65	72	26	255	25	-60	6	83.6	21.1	2.1
65	72	26	255	25	-60	6	83.6	21.1	2.1
65	72	26	255	25	-60	6	83.6	70.1	49.4
86	71	13	246	19	-41	6	78.8	75	50.5

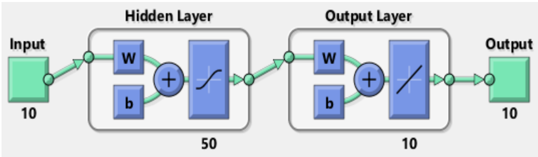

Figure 13. Structure of the Neural Network

Table 3. Sample of the test inputs

L_b	d_b	d_p	L_{22}	L_{23}	L_{42}	L_{43}	L_{62}	L_{63}	S_x
300	160	0	70	124	100	120	50	100	74.4
150	160	30	65	116	95	160	50	100	76.6
200	160	0	70	120	70	120	70	120	83.4
300	160	100	65	116	95	160	50	100	76.6
50	160	0	70	120	70	120	70	120	83.4
300	160	80	70	120	70	120	70	120	109.6

Table 4. Outputs given by the initial program for the test inputs

Z	α_{21}	α_{22}	α_{41}	α_{42}	α_{61}	α_{62}	W_x	MS_{-s}	MS_{-e}
80	75	14	223	16.5	-50	8	74.5	106.4	66.2
86	71	13	246	19	-41	6	78.8	50.6	28
65	72	26	255	25	-60	6	83.6	45.8	26.3
86	71	13	246	19	-41	6	78.8	103.5	85.5
65	72	26	255	25	-60	6	83.6	21.1	2.1
87	64	13	230	24.5	-60	6.5	110	113.1	39.7

5. RESULTS

The numeric program based on the theoretical equations makes it possible to simulate the performance of stability and possible displacement, by taking into account the equations of paragraph 3, which translate the constraints of stability and displacement. So, for any configuration, this program determines the margins of stability before and after a displacement, the possible movement and the effective distance that the robot will be able to cover. Consequently, if the configuration does not meet the requested performance, some parameters of the robot must be modified, such as the angles α_{ij}, in order to obtain a configuration which respects these performance characteristics and to obtain an optimal configuration, in terms of stability and possible displacement distance, depending on the desired travel distance. The program is validated by real configurations of the ants.

To directly obtain the optimal configurations, a resolution is made by an artificial intelligence program based on neural networks, by introducing the dimensional parameters of the robot, this program gives directly the optimal configuration, in particular the angles α_{ij} which ensure this optimal configuration.

A validity of the algorithm of the neural network is made by a test table, table 3, where there are other values of the inputs, the outputs of which are already given by the initial program are given in table 4. These values will be compared to the results obtained by the neural network algorithm given in table 5.

We conclude that the neural network algorithm gives very satisfactory results in comparison with the results of the numeric program, so this algorithm directly gives the optimal configurations.

Table 5. Outputs found by artificial intelligence

Z	α_{21}	α_{22}	α_{41}	α_{42}	α_{61}	α_{62}	W_x	MS_{-s}	MS_{-e}
80.0000014203576	74.9999994460503	13.9999999554671	222.999999954205	16.5000001598514	-49.9999992313534	7.99999996991612	74.5000033523189	106.399993707259	66.1999992458496
86.0000006300538	70.9999999016660	13.0000000314338	246.000000011584	19.0000000125651	-41.0000003399791	5.99999998725108	78.8000014254151	50.5999986992129	27.9999996391073
65.0000014550463	71.9999996368631	25.9999999065191	255.000000030017	25.0000002737325	-59.9999992635221	5.99999998254203	83.6000022491556	45.7999950701468	26.3000014989280
86.0000013810709	70.9999997734509	12.9999994797464	246.000000049049	19.0000001731336	-41.0000002125708	5.99999998494218	78.8000028124259	103.499996535797	85.4999989975358
65.0000000056915	72.0000003701285	26.0000009678143	254.999999306828	25.0000000221531	-60.0000002539205	5.99999995882917	83.5999999346609	21.0999984788024	2.10000677615550
87.0000022772869	63.9999999482536	13.0000007647298	229.999999352152	24.5000001788799	-59.9999992910290	6.49999999075054	110.000003998371	113.099990970332	39.6999989917190

6. CONCLUSION

The instability of the configurations causes effects on the movement of the robot, and variations in the level of the robot's body relative to the ground. This produces an irregularity of movement and can cause the robot to tip over. Although the lifting legs will block the tilts as they are about to become propelling legs, they will generate additional forces when are in contact with the ground.

The interference is also checked when a leg in lifting mode must not touch a leg that is in propelling. It is a condition that imposes the positioning distance of the leg 2, $S_x/2$ to be less than length $L_b/2$ of the robot's body.

This condition is well checked in the analysis of the insect case. Although the studied system (robot) has several parameters, an optimization is made, from the resolution carried out by a program and completed by a neural network algorithm, between possible displacement space (workspace), robot stability, the margins of stability and the desired displacement.

Thus, we observe that the neural network algorithm directly gives the optimized results, instead of numerically finding these results based on the theoretical equations. As a perspective, further analysis is needed to introduce the consumed energy and applied torques by the servomotors.

REFERENCES

[1] J. Linert, P. Kopacek, "Humanoid Robots Robotainment", IFAC-PapersOnLine, Vol. 51, No. 30, Art. No. 30, 2018.
[2] Z.G. Yang, M.L. Shao, D.I. Shin, "Kinematic Optimization of Parallel Manipulators with a Desired Workspace", AMM, Vol. 752-3, pp. 973-979, April 2015.
[3] E.G. Szadeczky Kardoss, Z. Gyenes, "Velocity Obstacles for Car Like Mobile Robots: Determination of Colliding Velocity and Curvature Pairs", Adv. Sci. Technol. Eng. Syst. J., Vol. 3, No. 1, Jan. 2018.
[4] J. Paskarbeit, et al., "Ourobot A Sensorized Closed Kinematic Chain Robot for 2021 Robotics and Auto", Robotics and Autonomous Systems. Vol. 140, June 2021.
[5] Z. Wang, H. Li, X. Zhang, "Construction waste Recycling Robot for Nails and Screws: Computer Vision Technology and Neural Network Approach", Automation in Construction, Vol. 97, pp. 220-228, January 2019.
[6] A. Dobrokvashina, R. Safin, Y. Bai, R. Lavrenov, "Improved Graphical User Interface for Crawler Robot Servosila Engineer", International Siberian Conference on Control and Communications (SIBCON), Kazan, Russia, pp. 1-5, May 2021.
[7] L. Bai, J. Guan, X. Chen, J. Hou, W. Duan, "An Optional Passive/Active Transformable Wheel Legged Mobility Concept for Search and Rescue Robots", Robotics and Autonomous Systems, Vol. 107, pp. 145-155, September 2018.
[8] S. Zhang, et al., "Design and Motion Analysis of Reconfigurable Wheel Legge 2021 Defense Techno", Defense Technology, p. S2214914721000751, April 2021.
[9] Q. Liu, X. Chen, B. Han, Z. Luo, X. Luo, "Virtual Constraint Based Control of Bounding Gait of Quadruped Robots", J. Bionic Eng., Vol. 14, No. 2, June 2017.
[10] L.W. Wang, W.W. Zhang, T.H. Wang, C.D. Wang, F.N. Meng, "Design and Simulation of a Single Leg of a Jumpable Bionic Robot with Joint Energy Storage Function", Procedia Computer Science, Vol. 166, pp. 315-322, 2020.
[11] Z. Zhang, L. Wang, J. Liao, J. Zhao, Z. Zhou, X. Liu, "Dynamic Stability of Bio Inspired Biped Robots for Lateral Jumping in Rugged Terrain", Applied Mathematical Modelling, Vol. 97, pp. 113-137, Sep. 2021.
[12] A.H.A. Al Dabbagh, R. Ronsse, "A Review of Terrain Detection Systems for Applications in Locomotion Assistance", Robotics and Autonomous Systems, Vol. 133, p. 103628, November 2020.
[13] W. Gouda, R.J.B. Chikha, "NAO Humanoid Robot Obstacle Avoidance Using Monocular Camera", Adv. Sci. Technol. Eng. Syst. J., Vol. 5, No. 1, Art. No. 1, Feb. 2020.
[14] B. Priyaranjan, et al., "Development of Quadruped Walking Robots", Ain Shams Engineering Journal, Vol. 12, No. 2, pp. 2017-2031, June 2021.
[15] T. Kobayashi, T. Sugino, "Reinforcement Learning for Quadrupedal Locomotion with Design of Continual-Hierarchical Curriculum", Engineering Applications of Artificial Intelligence, Vol. 95, p. 103869, October 2020.
[16] D. Xi, F. Gao, "Criteria of Type Complexity for Legged Robots", Mechanism and Machine Theory, Vol. 144, p. 103661, February 2020.
[17] J. Sun, J. Ren, Y. Jin, B. Wang, D. Chen, "Hexapod Robot Kinematics Modeling and Tripod Gait Design Based on the Foot end Trajectory", IEEE International Conference on Robotics and Biomimetics (ROBIO), Macau, pp. 2611-2616, December 2017.
[18] K. Xu, X. Ding, "Typical Gait Analysis of a Six-Legged Robot in the Context of Metamorphic Mechanism Theory", Chin. J. Mech. Eng., Vol. 26, No. 4, Art. No. 4, July 2013.
[19] E.H. Hasnaa, B. Mohammed, "Planning Tripod Gait of a Hexapod Robot", in 2017 14th International Multi-Conference on Systems, Signals & Devices (SSD), Marrakech, pp. 163-168, March 2017.
[20] A. Mahapatra, S.S. Roy, D.K. Pratihar, "Study on Feet Forces, Distributions, Energy Consumption and Dynamic Stability Measure of Hexapod Robot During Crab Walking", Applied Mathematical Modelling, Vol. 65, pp. 717-744, January 2019.
[21] G. Wang, L. Ding, H. Gao, Z. Deng, Z. Liu, H. Yu, "Minimizing the Energy Consumption for a Hexapod Robot Based on Optimal Force Distribution", IEEE Access, Vol. 8, pp. 5393-5406, 2020.
[22] M. Atify, M. Bennani, A. Abouabdellah, "Optimization of the Kinematics and Dynamics Performances of a Hexapod Robot", ISER International Conference, Kota Kinabalu, Malaysia, p. 7, 2021.
[23] X.Y. Sandoval Castro, M. Garcia Murillo, L.A. Perez Resendiz, E. Castillo Castaneda, "Kinematics of Hex-Piderix - A Six-Legged Robot - Using Screw Theory", p. 8, September 2012.
[24] X.Y. Sandoval Castro, E. Castillo Castaneda, "Statically Stable Adaptability Strategies to Terrain Change for a 6-Limbed Walking Robot", Rev. Iberoam. Autom. Inform. Ind., December 2018.
[25] R. Barrio, A. Lozano, M. Rodriguez, S. Serrano, "Numerical Detection of Patterns in CPGs: Gait Patterns in Insect Movement", Communications in Nonlinear Science and Numerical Simulation, Vol. 82, p. 105047, March 2020.
[26] R. Zhang, et al., "Structure Design and Traction Trafficability Analysis of Multi-Posture Wheel-Legs Bionic Walking Wheels for Sand Terrain", Journal of Terramechanics, Vol. 91, pp. 31-43, October 2020.
[27] Q. Chang, F. Mei, "A Bioinspired Gait Transition Model for a Hexapod Robot", Journal of Robotics, Vol. 2018, pp. 1-11, September 2018.
[28] Z. Zhang, D. Chen, K. Chen, H. Chen, "Analysis and Comparison of Two Jumping Leg Models for Bioinspired Locust Robot", J. Bionic Eng., Vol. 13, No. 4, Art. No. 4, December 2016.
[29] J. Zhang, J. Li, C. Li, Z. Wu, H. Liang, J. Wu, "Self-Righting Physiology of the Ladybird Beetle Coccinella Septempunctata on Surfaces with Variable Roughness", Journal of Insect Physi., Vol. 130, p. 104202, April 2021.
[30] G. Wang, X. Chen, S. Yang, P. Jia, X. Yan, J. Xie, "Subsea Crab Bounding Gait of Leg-Paddle Hybrid Driven Shoal Crablike Robot", Mechatronics, Vol. 48, pp. 1-11, December 2017.
[31] S. Zhang, J. Yao, Y. Wang, Z. Liu, Y. Xu, Y. Zhao, "Design and Motion Analysis of Reconfigurable Wheel-

Legged Mobile Robot", Defense Technology, p. S2214914721000751, April 2021.
[32] P. Biswal, P.K. Mohanty, "Development of Quadruped Walking Robots: A review", Ain Shams Engineering Journal, Vol. 12, No. 2, Art. No. 2, June 2021.
[33] R. Barrio, A. Lozano, M.A. Martinez, M. Rodriguez, S. Serrano, "Routes to Tripod Gait Movement in Hexapods", Neurocomputing, p. S0925231221007669, May 2021.
[34] H. Yu, H. Gao, Z. Deng, "Enhancing Adaptability with Local Reactive Behaviors for Hexapod Walking Robot via Sensory Feedback Integrated Central Pattern Generator", Robotics and Autonomous Systems, Vol. 124, p. 103401, February 2020.
[35] P. Billeschou, N.N. Bijma, L.B. Larsen, S.N. Gorb, J.C. Larsen, P. Manoonpong, "Framework for Developing Bio-Inspired Morphologies for Walking Robots", Applied Sciences, Vol. 10, No. 19, Art. No. 19, October 2020.
[36] M. Atify, M. Bennani, A. Abouabdellah, "Propelling Motion Modeling of a Hexapod Robot", The 1st International Conference on Smart Systems and DataScience (ICSSD), p. 5, 2019.
[37] F. Zha, C. Chen, W. Guo, P. Zheng, J. Shi, "A Free Gait Controller Designed for a Heavy Load Hexapod robot", Advances in Mechanical Engineering, Vol. 11, No. 3, Art. No. 3, March 2019.
[38] S.S. Roy, D.K. Pratihar, "Dynamic Modeling, Stability and Energy Consumption Analysis of a Realistic Six-Legged Walking Robot", Robotics and Computer Integr. Manufac., Vol. 29, No. 2, Art. No. 2, April 2013.
[39] E. Garcia, J. Estremera, P.G. de Santos, "A Comparative Study of Stability Margins for Walking machines", Robotica, Vol. 20, No. 6, Art. No. 6, November 2002.
[40] D. Wojtkowiak, I. Malujda, K. Talaska, L. Magdziak, B. Wieczorek, "Influence of Construction Mass Distribution on the Walking Robot's Gait Stability", Procedia Engineering, Vol. 177, pp. 419-424, 2017.
[41] T.T. Lee, C.M. Liao, T.K. Chen, "On the Stability Properties of Hexapod Tripod Gait", IEEE J. Robot. Automat., Vol. 4, No. 4, Aug. 1988.
[42] S.S. Roy, D.K. Pratihar, "Effects of Turning Gait Parameters on Energy Consumption and Stability of a Six-Legged Walking Robot", Robotics and Autonomous Systems, Vol. 60, No. 1, January 2012.
[43] E. Garcia, P.G. de Santos, "A New Dynamic Energy Stability Margin for Walking Machines", p. 7, July 2003.
[44] M. Agheli, Stephen. S. Nestinger, "Force-Based Stability Margin for Multi-Legged Robots", Robotics and Autonomous Systems, Vol. 83, pp. 138-149, Sep. 2016.
[45] M. Agheli, S.S. Nestinger, "Study of the Foot Force Stability Margin for Multi-Legged Wheeled Robots Under Dynamic Situations", The 8th IEEE/ASME International Conference on Mechatronic and Embedded Systems and Applications, Suzhou, China, pp. 99-104, July 2012.
[46] M. Atify, M. Bennani, A. Abouabdellah, "Workspace of a Hexapod", International Journal on Technical and Physical Problems of Engineering (IJTPE), Issue 48, Vol. 13, No. 3, pp. 25-34, September 2021.
[47] M.M.A. Hajiabadi, "Analytical Workspace, Kinematics, and Foot Force Based Stability of Hexapod Walking Robots", pp. 34-42, May 2013.
[48] https://www.youtube.com/watch?v=tWHnT08wU1o, consulted in August 13, 2021.
[49] https://www.youtube.com/watch?v=IHEYBvriv2I, consulted in August 13, 2021.
[50] https://www.youtube.com/watch?v=318H8p7GuB8, consulted in July 2021.
[51] http://antsofthecape.blogspot.com/p/ants-up-to-about-5-mm-long.html, November 2021.
[52] E.H. Hssayni, M. Ettaouil, "Generalization Ability Augmentation and Regularization of Deep Convolution Neural Networks Using $l^{1/2}$ Pooling", International Journal on Technical and Physical Problems of Engineering (IJTPE), Issue 48, Vol. 13, No. 3, pp. 1-6, September 2021.
[53] A. Bellat, K. Mansouri, A. Raihani, "Implementation of Artificial Neural Network for Optimization of a Wind Farm", International Journal on Technical and Physical Problems of Engineering (IJTPE), Issue 47, Vol. 13, No. 2, pp. 35-39, June 2021.

BIOGRAPHIES

Mohamed Atify was born in Morocco. He received the mechanical aggregation from Technical School (ENSET), Rabat, Morocco in 1998. He obtained master in mechanical engineering from technical school, Mohammed V University, Rabat, Morocco, 2016. He is currently working toward his Ph.D. in robotics, laboratory of systems engineering in Ibn Tofail University, Kenitra, Morocco. His research is focused on modeling, simulation & control of hexapod robots.

Mohammed Bennani was born in Morocco. He is a Professor in Robotics and Control of Dynamical Systems at ENSET Engineering School, University Mohammed V, Rabat, Morocco. He received the Doctorate degree from EMI Rabat School, Rabat, Morocco, in 1997, and Master in Robotics from University of Montpellier, France, in 1990. His research interests are modeling and control in robotics, motion & stability of celestial objects.

Abdellah Abouabdellah was born in Roummani, Morocco in 1968. He obtained the Doctor of Science-Applied in 2010 from Mohammed V University, Rabat, Morocco. He is a member of the energy team intelligent, electrical, industrial, attached to laboratory Systems Engineering at University of IbnTofail, Kenitra, Morocco. Currently, he is Professor research at the National School of Applied Sciences, Kenitra, Morocco. He is also coordinator of the engineering sector in industrial and logistics engineering. He is the author, co-author of several articles in journals, national and international conferences. His research is the modeling of business processes, predictions systems and logistics.